Electronic Supplementary Material (ESI) for Physical Chemistry Chemical Physics.

Extended Conjugation of ESIPT-Type Dopants in Nematic Liquid Crystalline Phase for Enhancing Fluorescence Efficiency and Anisotropy

Wanying Zhang,[a] Satoshi Suzuki,[b] Tsuneaki Sakurai,*[a,c] Hiroyuki Yoshida,[d]
Yusuke Tsutsui, [a] Masanori Ozaki, [d] and Shu Seki*[a]

[a.] Department of Molecular Engineering, Kyoto University, Nishikyo-ku, Kyoto 615-8510, Japan.

[b.] Fukui Institute for Fundamental Chemistry, Kyoto University, Kyoto 606-8103, Japan.

[c.] Faculty of Molecular Chemistry and Engineering, Kyoto Institute of Technology, Hashikami-cho, Matsugasaki, Sakyo-ku, Kyoto 606-8585, Japan.

[d.] Division of Electrical, Electronic and Infocommunications Engineering, Osaka University, 2-1 Yamadaoka, Suita, Osaka 565-0871, Japan.

*Correspondence: sakurai@kit.ac.jp, seki@moleng.kyoto-u.ac.jp

General Methods

All the chemicals were purchased from Tokyo Chemical Industry Co., Wako Pure Chemical Co. (FUJIFILM), and Sigma-Aldrich Co. (Merck), and used as received. TLC analyses were carried out on aluminum sheets coated with silica gel 60 (Merck). Column chromatography was performed on Silica Gel 60N (spherical, neutral) from Kanto Chemicals Industry Co. ^{1}H NMR and ^{13}C NMR spectra were recorded in $CDCl_3$ on a JEOL model AL-400 spectrometer, operating at 400 and 100 MHz, respectively, where chemical shifts were determined with respect to tetramethylsilane (TMS, δ 0.00) or $CHCl_3$ as an internal reference. High-resolution electrospray ionization (ESI) mass spectrometry was performed on a Thermo Fisher Scientific Exactive Plus Orbitrap mass spectrometer with an Ultimate 3000 high-performance liquid chromatography system.All the mixtures of **5CB/C$_5$P-C≡C-HBT** and **5CB/C$_8$P-C≡C-HBT** were prepared in the glass vial at corresponding weight ratios. Each mixture was heated to 150°C to give transparent homogenous mixtures and allowed to cool to room temperature. The optical textures were recorded by an Olympus BX53-P polarizing optical microscope (POM) equipped with a Mettler HS82 hot-stage system, where the sample was loaded into a 5-μm thick sandwiched glass cell without surface treatment. DSC measurements were proceeded on a Perkin Elmer DSC8000 differential scanning calorimeter. XRD experiments of the mixtures were carried out using a Rigaku MiniFlex600 X-ray diffractometer (λ = 1.54 Å) with a D/teX Ultra semiconductor detector and a Rigaku HPC hot stage equipped with a temperature controller. Electronic absorption spectra were recorded on a JASCO V-570 spectrometer. Polarizing absorption spectra were carried out using a WP25M-UB mounted wire grid polarizer (φ ~25 mm). Absorbance difference spectra were detected by Avaspec2048 with the light source LC8 and the voltage was applied by a NF Corporation WF1973 function generator. Fluorescence spectra were measured on a JASCO FP-8500 fluorescence spectrophotometer. Absolute fluorescence quantum yields (Φ_{FL}) were evaluated on this spectrometer with a JASCO ILF-835 fluorescence integrate sphere unit. Fluorescence lifetimes were estimated upon photoexcitation at 355 nm by picosecond pulse train (~7 ps pulse width, 1 kHz repetition, ~140 nW) from a EKSPLA PL2250 Nd:YVO_4 laser. Fluorescence light was corrected and guided into a Hamamatsu C5094 monochromator, and then picked by a Hamamatsu C4334 streak scope equipped with a micro-channel plate. The slit width of monochromator was adjusted to 200 μm corresponding to the wavelength resolution of 12 nm. Fluorescence decay profiles were obtained by averaging 20 nm range around the peak wavelength. The measurements were performed using bulk crystals for **C$_5$P-C≡C-HBT** and **5CB/C$_5$P-C≡C-HBT** (95/5 wt/wt) in a 1 × 1 cm quartz cell.

Quantum Chemical Calculation

Potential energy profiles of **HBT** and **HP-C≡C-HBT** were obtained with time-dependent density functional theory (TDDFT) including solvent effects as a polarized continuum model (PCM). Geometries of local minima and transition states were optimized with TD-CAM-B3LYP/6-311++(d,p) using Gaussian 16 program.[S1] Geometry of minimum energy conical intersections were optimized with spin-flip (SF) TD-BHHLYP/6-31G(d) in vacuo using branching plane updating method[S2] in GAMESS,[S3] and then single-point

calculations were performed with TD-CAM-B3LYP/6-311++(d,p) with PCM using Gaussian 16.

Polarizing Fluorescence Microscopy

Fluorescence anisotropy was evaluated by micro-spectroscopy of polarized fluorescence. Glass sandwich cells with a cell-gap of 5 μm and parallel rubbing treatment on both substrates were purchased from EHC Co., Japan. A **5CB/C_5P-C≡C-HBT** mixture was injected in the cell by capillary action, and the sample was observed under a Nikon Eclipse LV100N-POL POM with fluorescence measurement capability. Non-polarized light (λ_{ex} ~365 nm) from an Ushio SP-9 high-pressure mercury lamp was introduced into the microscope using a bundled optical fiber and irradiated on the sample through a Nikon UV-2A fluorescence cube and a ×10 objective lens. The emitted fluorescence spectrum was measured using a Hamamatsu PMA-12 spectrometer after passing through the emission filter of the same cube and a polarizer (referred to as analyzer). The excitation spot had a hexagonal geometry with a side of 150 μm.

Synthesis

The target compounds, **C_5P-C≡C-HBT** and **C_8P-C≡C-HBT**, were synthesized as shown in Scheme 1. To a THF/Et_3N (30 ml, 1/1 v/v) solution of **I-HBT**[S4] (1.0 g, 2.8 mmol), $Pd(PPh_3)_4$ (0.33 g, 0.28 mmol), CuI (0.16 g, 0.85 mmol) and 1-ethynyl-4-pentylbenzene (or 1-ethynyl-4-octylbenzene) (2.8 mmol) were added under N_2, and the reaction mixture was degassed via freeze-pump-thaw cycles for three times. The mixture was stirred for 12 h at 25°C, filtered through Celite® from insoluble fractions, and evaporated to dryness under reduced pressure. The obtained solid was purified by silica gel column chromatography with an eluent of hexane/dichloromethane (2/1 v/v). The collected fraction was evaporated to dryness under reduced pressure, and then recrystallized from hexane, affording pale yellow crystals. Yield: 45% for **C_5P-C≡C-HBT** (0.51 g, 1.3 mmol) and 61% for **C_8P-C≡C-HBT** (0.76 g, 1.7 mmol).

C_5P-C≡C-HBT: ^{1}H NMR ($CDCl_3$): 12.59 (s, 1H, OH), 7.99 (d, *J* = 7.8 Hz, 1H, Ar-H), 7.91 (d, *J* = 7.8 Hz, 1H, Ar-H), 7.54 (d, *J* = 7.8 Hz, 1H, Ar-H), 7.47 (dq, *J* = 7.6 Hz, 5H, Ar-H), 7.18 (d, *J* = 8.3 Hz, 2H, Ar-H), 7.10 (dd, *J* = 8.0 Hz, 1H, Ar-H), 2.64–2.61 (t, 2H, CH_2), 1.67–1.58 (m, 2H, CH_2), 1.34–1.32 (t, 4H, CH_2), 0.90 (t, *J* = 7.1 Hz, 3H, CH_3). ^{13}C NMR ($CDCl_3$): 168.69, 157.65, 151.80, 143.97, 132.65, 131.69, 128.54, 128.26, 127.75, 126.82, 125.66, 122.77, 122.22, 121.53, 120.52, 119.91, 116.54, 92.10, 88.33, 35.88, 31.49, 30.94, 22.54, 13.99. ESI-HRMS (m/*z*): calcd. for $[M - H]^-$ 396.1428, obsd. 396.1423.

C_8P-C≡C-HBT: 1H NMR ($CDCl_3$): 12.60 (s, 1H, OH), 8.00 (d, *J* = 7.8 Hz, 1H, Ar-H), 7.93 (d, *J* = 8.8 Hz, 1H, Ar-H), 7.66 (d, *J* = 8.3 Hz, 1H, Ar-H), 7.48 (dq, *J* = 7.6 Hz, 5H, Ar-H), 7.19 (d, *J* = 7.8 Hz, 2H, Ar-H), 7.11 (d, *J* = 8.3 Hz, 1H, Ar-H), 2.65–2.61 (t, 2H, CH_2), 1.65–1.59 (m, 2H, CH_2), 1.32–1.28 (d, 4H, CH_2), 0.89 (t, *J* = 6.6 Hz, 3H, CH_3). ^{13}C NMR ($CDCl_3$): 168.69, 157.66, 151.81, 143.97, 132.65, 131.69, 128.55, 128.26, 127.76, 126.82, 125.67, 122.77, 122.26, 121.56, 120.54, 119.91, 116.57, 92.11, 35.95, 31.88, 31.24, 29.44, 29.24, 22.67, 14.10. ESI-HRMS (m/*z*): calcd. for $[M - H]^-$ 438.1897, obsd. 438.1893.

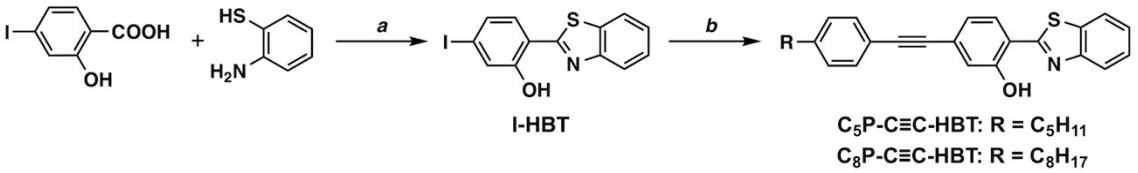

Scheme 1. Synthetic route of **C_5P-C≡C-HBT** and **C_8P-C≡C-HBT**. Conditions: (a) PCl_3, toluene, reflux, 10 h; (b) 4-ethynyl-1-pentylbenzene or 4-ethynyl-1-octylbenzene, $Pd(PPh_3)_4$, CuI, THF, Et_3N, 25°C, 12 h.

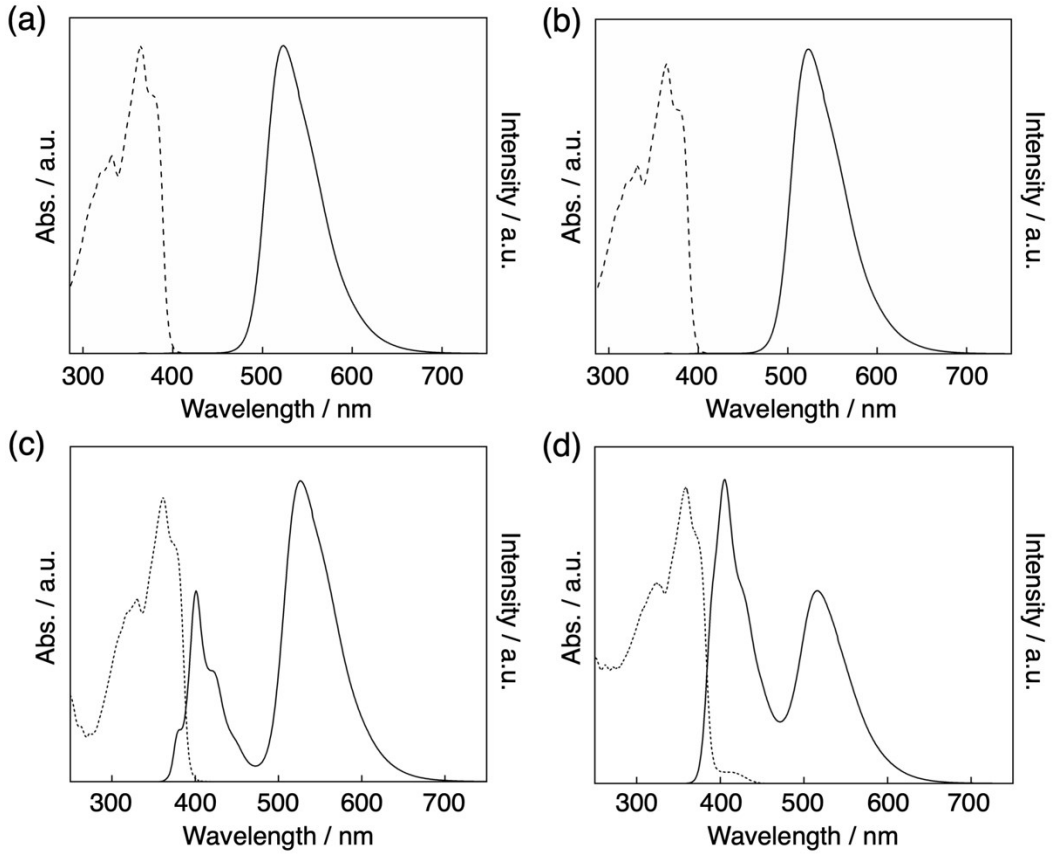

Figure S1. Absorption (dashed) and fluorescence (solid) spectra of (a) **C_5P-C≡C-HBT** and (b) **C_8P-C≡C-HBT** in toluene at 50 μM. Fluorescence spectra of **C_5P-C≡C-HBT** in (c) THF and (d) EtOH at 50 μM.

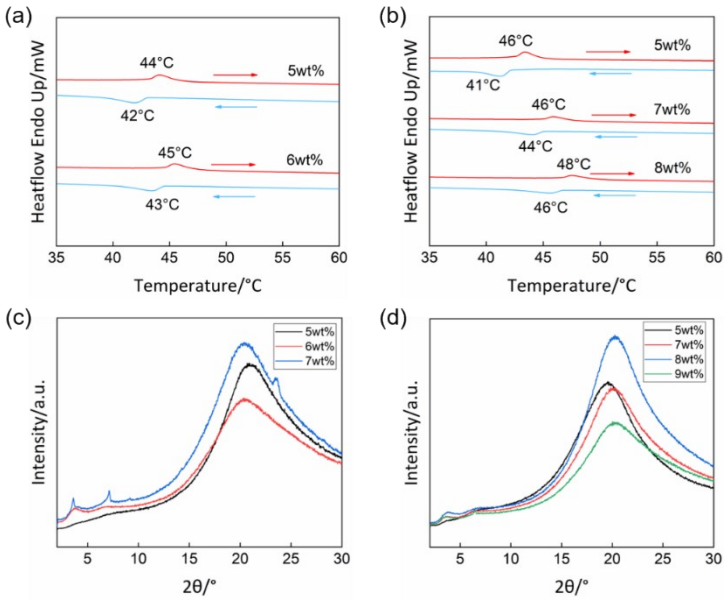

Figure S2. DSC profiles of (a) 5CB/**C_5P-C≡C-HBT** and (b) 5CB/**C_8P-C≡C-HBT**. XRD patterns of (c) 5CB/**C_5P-C≡C-HBT** and (d) 5CB/**C_8P-C≡C-HBT** at different weight ratios.

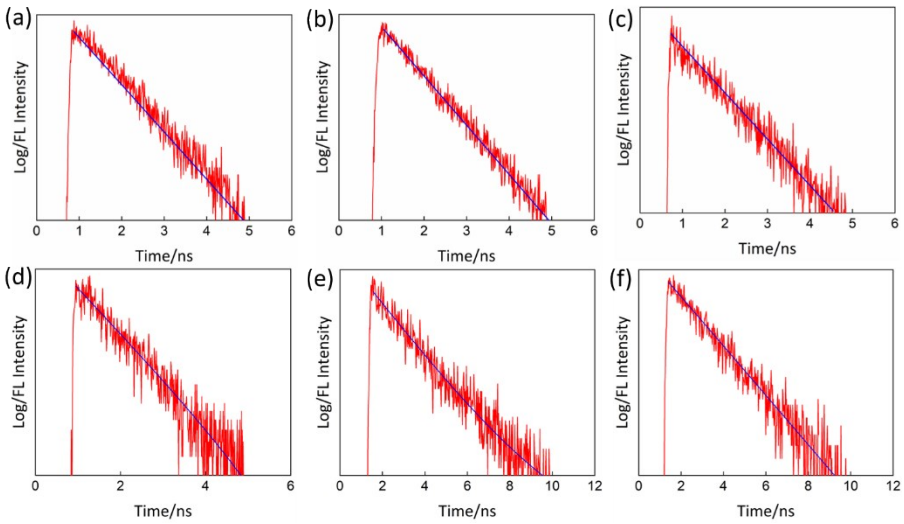

Figure S3. Fluorescence decay profiles (red) and fitted lines (blue) of (a) CH_2Cl_2 solution (500 μM) of **C_5P-C≡C-HBT** at 515 nm, (b) **C_5P-C≡C-HBT** in crystal phase at 523 nm, and (c) 5CB/**C_5P-C≡C-HBT** (95/5 w/w) at 528 nm; (d) CH_2Cl_2 solution (500 μM) of **C_8P-C≡C-HBT** at 522 nm, (e) **C_8P-C≡C-HBT** in crystal phase at 530 nm, and (f) 5CB/**C_8P-C≡C-HBT** (95/5 w/w) at 528 nm at 25°C with λ_{ex} = 355 nm.

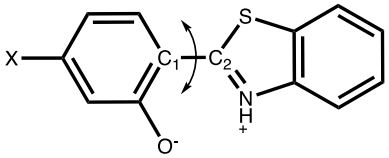

Figure S4. Numbering of carbon atoms in HBT structure.

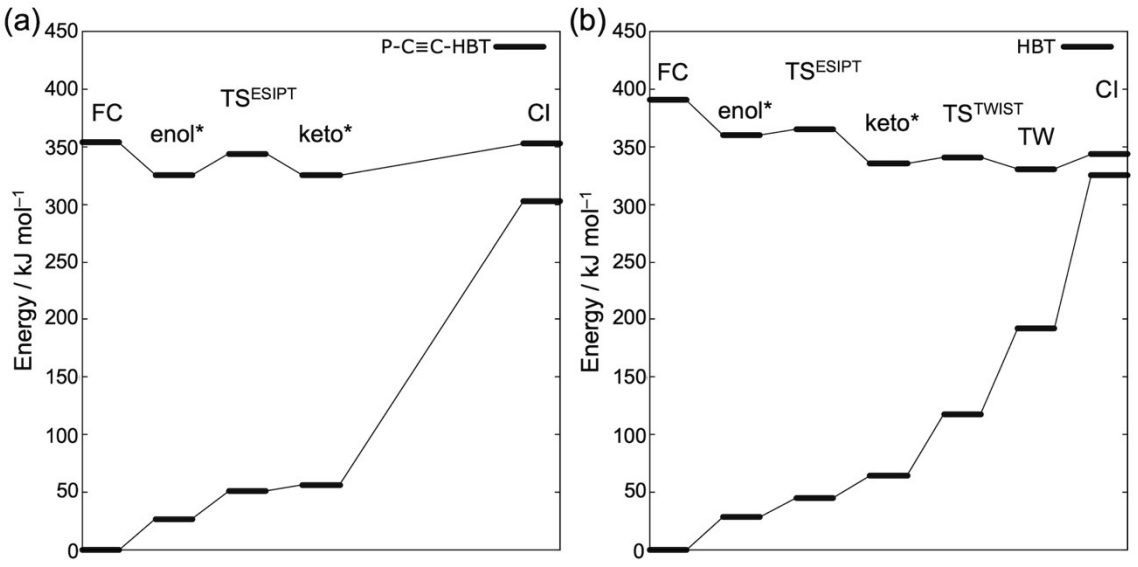

Figure S5. Energy profiles for non-radiative decay processes of (a) **P-C≡C-HBT** and (b) HBT in toluene calculated by PCM/TD-CAM-B3LYP/6-311+G(d,p)//SFTD-BHHLYP/6-311+G(d). FC: Frank-Condon state, TS: transition state, TW: twisted state, CI: conical intersection.

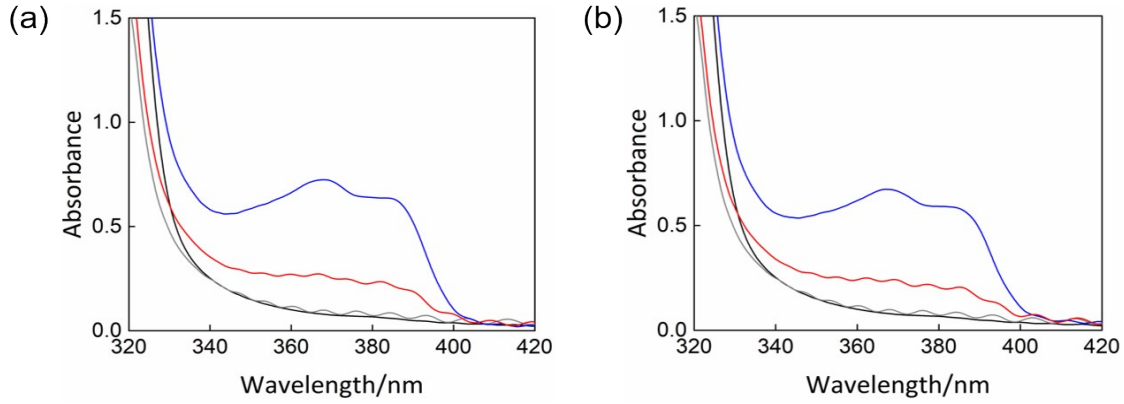

Figure S6. Polarized absorption spectra of 5CB (black, gray) and (a) 5CB/**C_5P-C≡C-HBT**, (b) 5CB/**C_8P-C≡C-HBT** (99.3/0.7 w/w) (red, blue) in a 5-μm ITO coated glass cell. The incident light was polarized in parallel (black, blue) and perpendicular (gray, red) to the rubbing direction of polyimide surfaces on the glass.

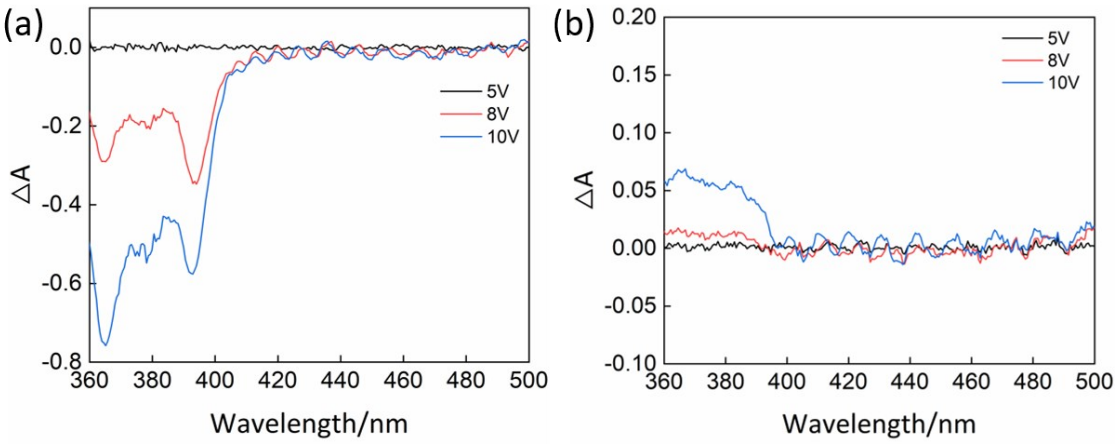

Figure S7. Absorbance difference spectra with polarized incident light of 5CB/ **C_5P-C≡C-HBT** (95/5 w/w) in 5-μm ITO-coated cell at (a) 0° and (b) 90° relative to the direction of the rubbing cell under different applied voltage.

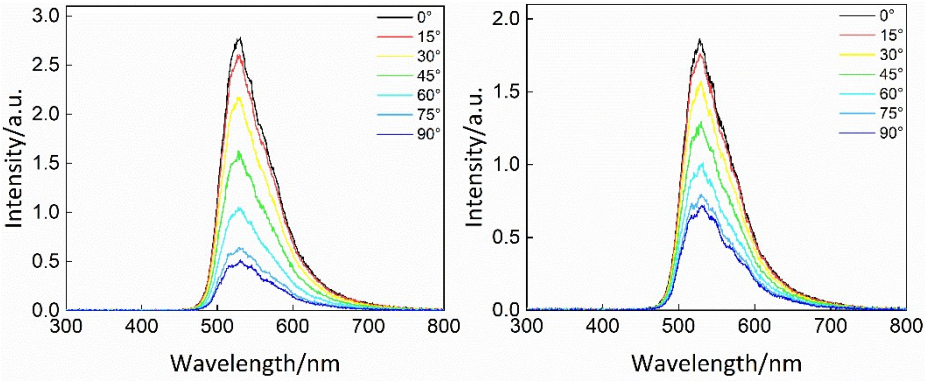

Figure S8. Polarized fluorescence spectra of 5CB/**C_5P-C≡C-HBT** (95/5 w/w) in 5-μm ITO coated cell with antiparallel rubbing treatment of polyimide surface under polarized excitation light at 0° (left) and 90° (right).

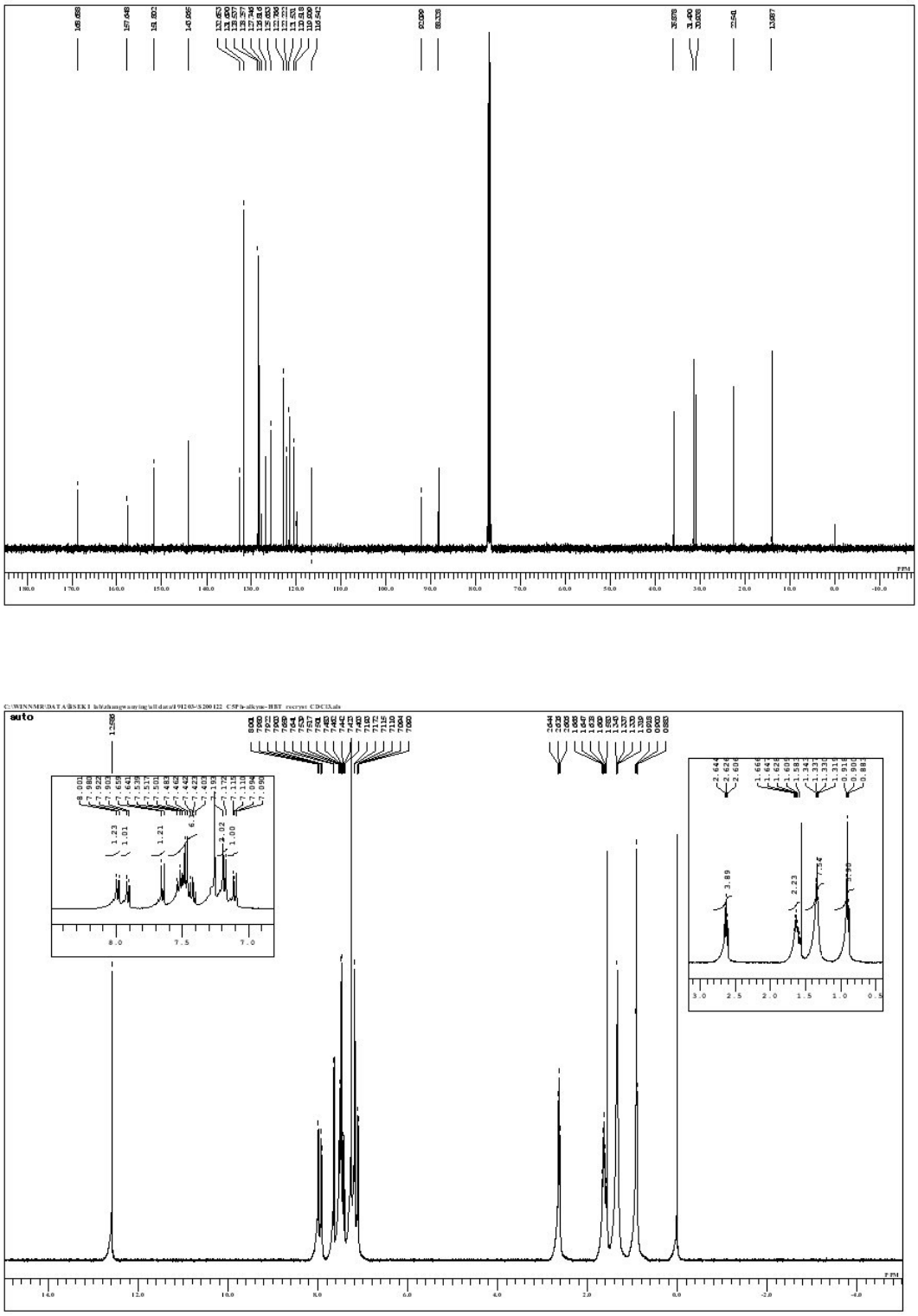

Figure S9. ^{13}C (top) and ^{1}H (bottom) NMR spectra of **C_5P-C≡C-HBT** in $CDCl_3$.

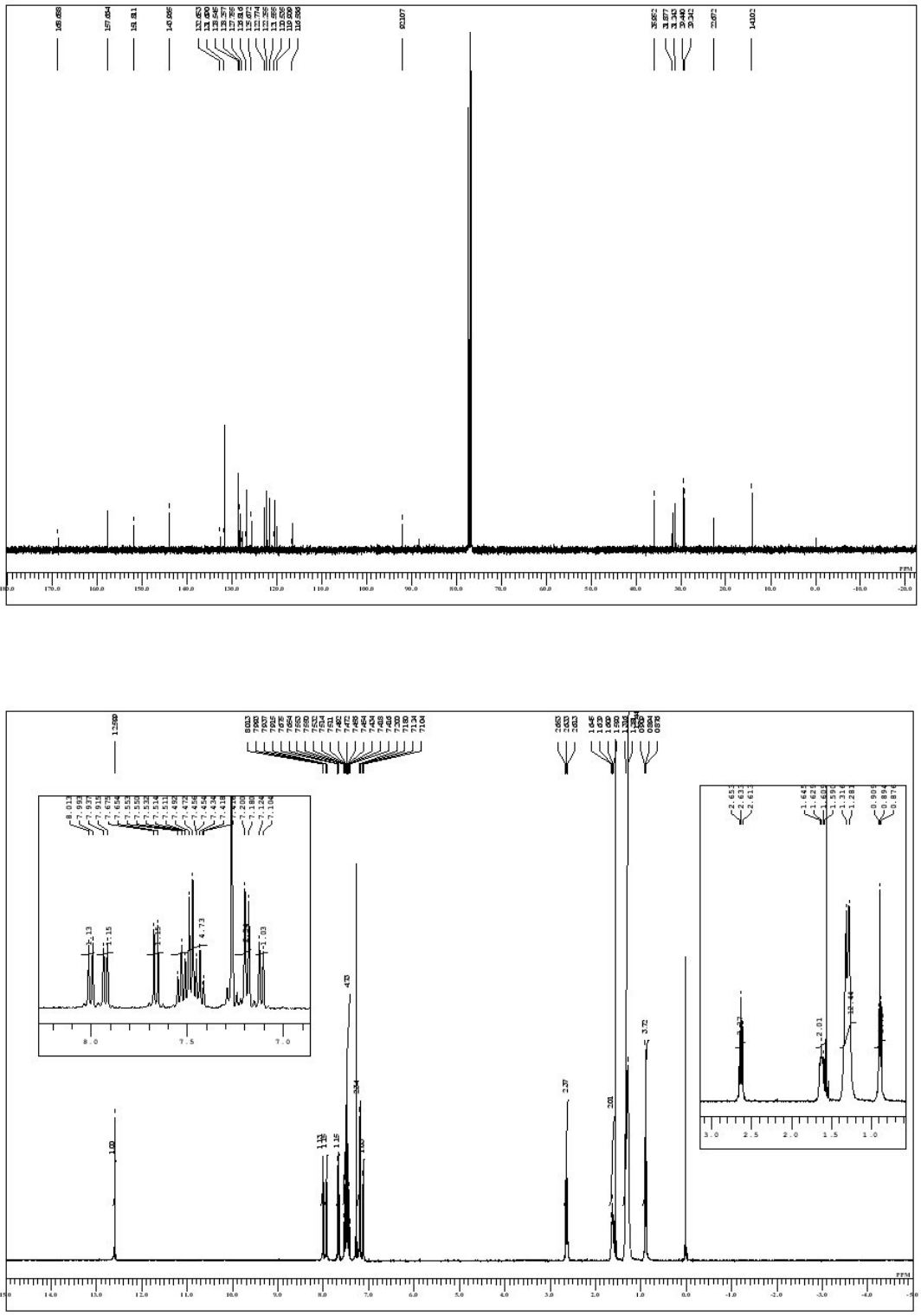

Figure S10. ^{13}C (top) and ^{1}H (bottom) NMR spectra of **C_8P-C≡C-HBT** in $CDCl_3$.

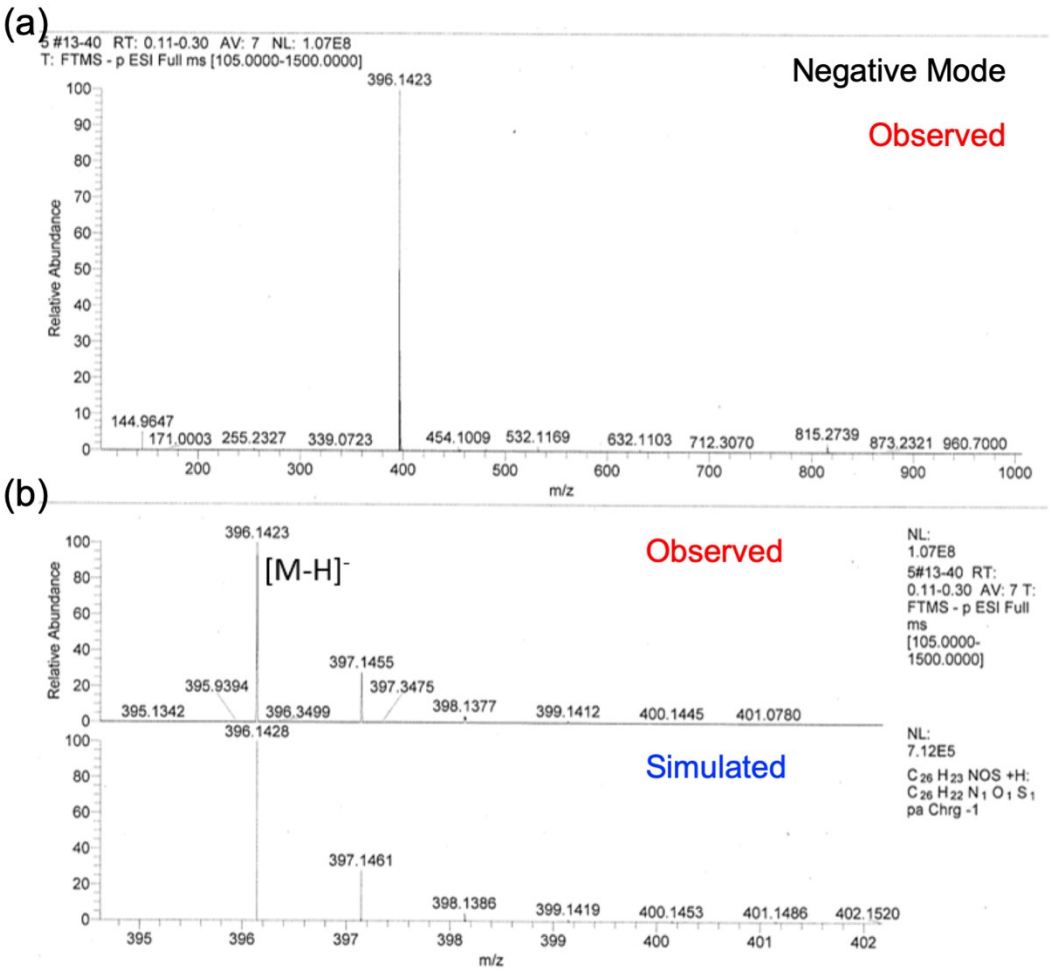

Figure S11. (a) ESI-TOF-MS spectra and (b) its magnified view of **C_5P-C≡C-HBT** in negative mode. Simulated isotope pattern was shown in (b).

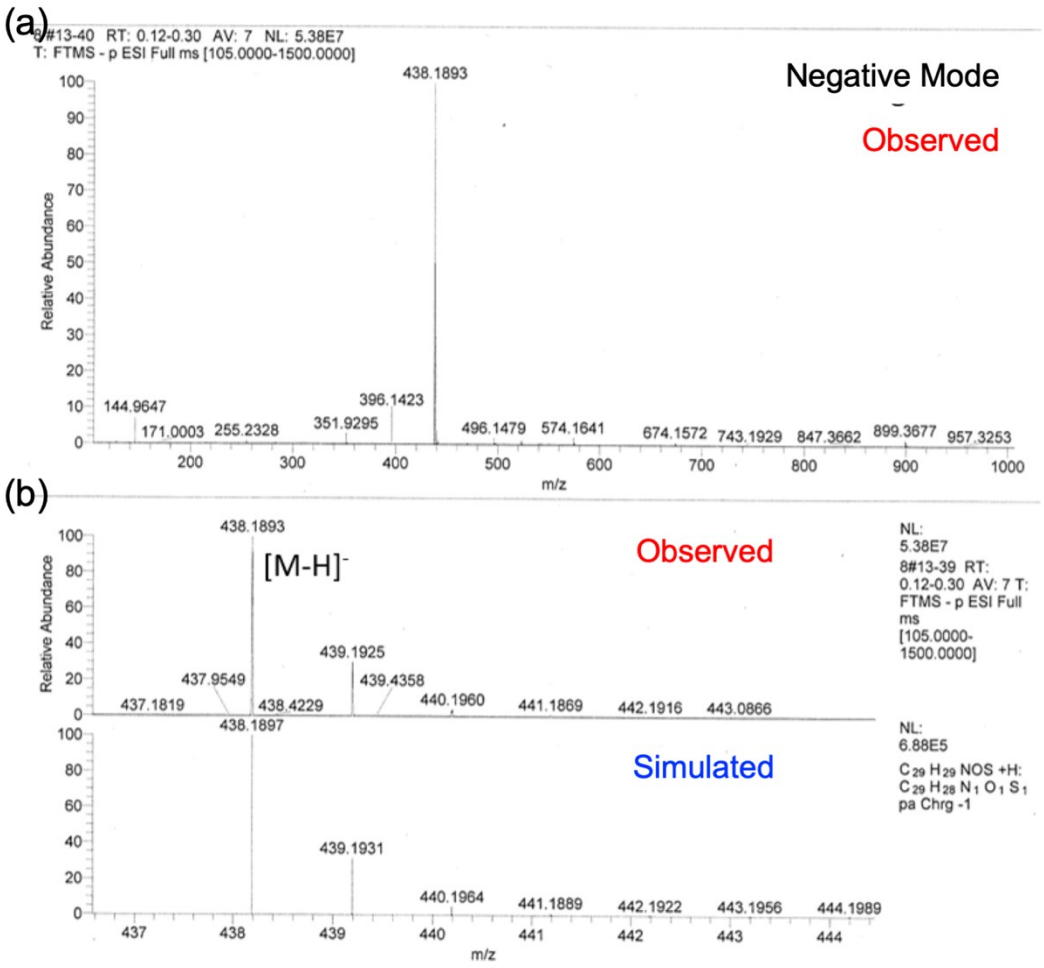

Figure S12. (a) ESI-TOF-MS spectra and (b) its magnified view of **C_8P-C≡C-HBT** in negative mode. Simulated isotope pattern was shown in (b).

References

S1 M. J. Frisch, G. W. Trucks, H. B. Schlegel, G. E. Scuseria, M. A. Robb, J. R. Cheeseman, G. Scalmani, V. Barone, G. A. Petersson, H. Nakatsuji, X. Li, M. Caricato, A. V. Marenich, J. Bloino, B. G. Janesko, R. Gomperts, B. Mennucci, H. P. Hratchian, J. V. Ortiz, A. F. Izmaylov, J. L. Sonnenberg, D. Williams-Young, F. Ding, F. Lipparini, F. Egidi, J. Goings, B. Peng, A. Petrone, T. Henderson, D. Ranasinghe, V. G. Zakrzewski, J. Gao, N. Rega, G. Zheng, W. Liang, M. Hada, M. Ehara, K. Toyota, R. Fukuda, J. Hasegawa, M. Ishida, T. Nakajima, Y. Honda, O. Kitao, H. Nakai, T. Vreven, K. Throssell, J. A. Montgomery, Jr., J. E. Peralta, F. Ogliaro, M. J. Bearpark, J. J. Heyd, E. N. Brothers, K. N. Kudin, V. N. Staroverov, T. A. Keith, R. Kobayashi, J. Normand, K. Raghavachari, A. P. Rendell, J. C. Burant, S. S. Iyengar, J. Tomasi, M. Cossi, J. M. Millam, M. Klene, C. Adamo, R. Cammi, J. W. Ochterski, R. L. Martin, K. Morokuma, O. Farkas, J. B. Foresman and D. J. Fox, Gaussian, Inc., Wallingford CT, 2016.

S2 S. Maeda, K. Ohno and K. Morokuma, *J. Chem. Theory Comput.*, 2010, **6**, 1538–1545.

S3 M. W. Schmidt, K. K. Baldridge, J. A. Boatz, S. T. Elbert, M. S. Gordon, J. H. Jensen, S. Koseki, N. Matsunaga, K. A. Nguyen, S. Su, T. L. Windus, M. Dupuis and J. A. Montgomery, *J. Comput. Chem.*, 1993, **14**, 1347–1363.

S4 W. Zhang, T. Sakurai, M. Aotani, G. Watanabe, H. Yoshida, V. S. Padalkar, Y. Tsutsui, D. Sakamaki, M. Ozaki and S. Seki, *Adv. Opt. Mater.*, 2019, **7**, 1801349.